New Open-Framework Zinc Oxalates Synthesized in the Presence of Structure-Directing Organic Amines

R. Vaidhyanathan,[†] Srinivasan Natarajan,[†] Anthony K. Cheetham,*[,‡] and C. N. R. Rao*[,†]

Chemistry and Physics of Materials Unit, Jawaharlal Nehru Centre for Advanced Scientific Research, Jakkur P.O., Bangalore 560 064, India, and Materials Research Laboratory, University of California, Santa Barbara, California 93106

Received July 12, 1999. Revised Manuscript Received September 15, 1999

Two new open-framework zinc oxalates have been prepared by hydrothermal methods in the presence of structure-directing organic amines. The crystal data for these oxalates are as follows: **I**, $[H_3N(CH_2)_3NH_3]^{2+}[Zn_2(C_2O_4)_3]^{2-}\cdot 3H_2O$, triclinic, space group $P\bar{1}$ (no. 2), a = 9.261(1) Å, b = 9.455(1) Å, c = 12.487(1), α = 83.93(1)°, β = 88.01(1)°, γ = 61.03(1)°, V = 951.1(1) Å^3, Z = 2, M = 524.8, D_{calc} = 1.83 g cm^{-3}, μ = 2.60 mm^{-1}, Mo Kα, R_F = 0.03; **II**, $2[C_3H_7NH_3]^{+}[Zn_2(C_2O_4)_3]^{2-}\cdot 3H_2O$, monoclinic, space group $C2/c$ (no. 15), a = 15.847(1) Å, b = 9.685(1) Å, c = 18.333(1), β = 115.5(1)°, V = 2539.1(2) Å^3, Z = 4, M = 569.1, D_{calc} = 1.60 g cm^{-3}, μ = 1.97 mm^{-1}, Mo Kα, R_F = 0.07. In **I**, the linkages between the Zn and oxalate units gives rise to a layered architecture with 12-membered (6 Zn and 6 oxalates) honeycomb-like apertures wherein the amine and water molecules are located. In **II**, the Zn−oxalate layers are cross-linked by another oxalate unit giving rise to a three-dimensional structure with two distinct channels where the amine and water molecules reside; the largest aperture in **II** involves a 20-membered ring (10 Zn and 10 oxalates). There is extensive hydrogen bonding among the amine, water, and the framework. Adsorption studies indicate that water can be reversibly adsorbed in **I**.

Introduction

Inorganic open-framework materials, in particular those formed by metal phosphates, have been investigated widely during the past decade.[1] The open-framework metal phosphates are generally synthesized hydrothermally in the presence of organic amines. In the past few years there has been considerable effort in designing open-framework inorganic materials other than phosphates, such as chalcogenides, pnictides, cyanides, and thiopnictides.[2] There has been some success with open-framework structures formed by metal carboxylates[3−5] wherein the carboxylates cross-link the extended metal−oxygen networks made from edge- and/or corner-shared polyhedra, giving rise to a three-dimensional connectivity possessing channels. These materials somewhat resemble the channel structures formed by the phosphates, but they have been prepared in the absence of any organic amines. The recent report of novel tin(II) oxalates with open architecture synthesized in the presence of structure-directing amines (SDA's)[6,7] led us to explore the possibility of designing new open-framework carboxylate structures, by carrying out hydrothermal synthesis in the presence of SDA's. In this direction, we have carried out the synthesis of zinc oxalates in the presence of organic amines. Although transition metal oxalates with layered and other architectures containing amines have been reported,[8,9] to our knowledge, open-framework zinc oxalates of well-defined structures have not been reported hitherto. It is generally assumed that zinc oxalates may also form honeycomb structures.[8] In this paper, we report the hydrothermal synthesis of two new Zn oxalates, $[H_3N(CH_2)_3NH_3]^{2+}[Zn_2(C_2O_4)_3]^{2-}\cdot 3H_2O$ (**I**) and $2[C_3H_7NH_3]^{+}[Zn_2(C_2O_4)_3]^{2-}\cdot 3H_2O$ (**II**). These oxalates contain 12- and 20-membered rings with the amine and water molecules residing in the pores. While **I** possess layers with honeycomb-like 12-member pores within the layers, **II** has a three-dimensionally extended network formed by cross-linked 20-membered pores with an interrupted honeycomb structure. The occur-

* Corresponding author. E-mail: cnrrao@jncasr.ac.in.
[†] Jawaharlal Nehru Centre for Advanced Scientific Research.
[‡] University of California, Santa Barbara.

(1) Cheetham, A. K.; Férey, G.; Loiseau, T. *Angew. Chem*. **1999** in press. Thomas, J. M. *Angew. Chem., Int. Ed. Engl*. **1994**, *33*, 913. Thomas, J. M. *Chem. Eur. J*. **1997**, *3*, 1557.
(2) Bowes, C. L.; Ozin, G. A. *Adv. Mater*. **1996**, *8*, 13. Conrad, O.; Jansen, C.; Krebs, B. *Angew. Chem., Int. Ed*. **1998**, *37*, 3208.
(3) Romero, S.; Mosset, A.; Trombe, J. C. *Eur. J. Solid State Inorg. Chem*. **1997**, *34*, 209. Kiritsis, V.; Michaelides, A.; Skoulika, S.; Golhen, S.; Ouahab, L. *Inorg. Chem*. **1998**, *37*, 3407.
(4) Serpaggi, F.; Férey, G. *J. Mater. Chem*. **1998**, *8*, 2749; **1998**, *8*, 2737. Livage, C.; Egger, C.; Nogues, M.; Férey, G. *J. Mater. Chem*. **1998**, *8*, 2743.
(5) Livage, C.; Egger, C.; Férey, G. *Chem. Mater*. **1999**, *11*, 1546.
(6) Ayyappan, S.; Cheetham, A. K.; Natarajan, S.; Rao, C. N. R. *Chem. Mater*. **1998**, *10*, 3746.
(7) Natarajan, S.; Vaidhyanathan, R.; Rao, C. N. R.; Ayyappan, S.; Cheetham, A. K. *Chem. Mater*. **1999**, *11*, 1633.
(8) Decurtins, S.; Schmalle, H. W.; Oswald, H. R.; Linden, A.; Ensling, J.; Gütlich, P.; Hauser, A. *Inorg. Chem*. **1993**, *32*, 1888 and the references therein; *J. Am. Chem. Soc*. **1994**, *116*, 9521.
(9) Tamaki, H.; Zhong, Z. J.; Matsumoto, N.; Kida, S.; Koikawa, M.; Achiwa, N.; Hashimoto, Y.; Okawa, H. *J. Am. Chem. Soc*. **1992**, *114*, 6974. Mathoniere, C.; Carling, S. G.; Day, P. *J. Chem. Soc., Chem. Commun*. **1994**, 1551. Clemente-Leon, M.; Coronado, E.; Galán-Mascarós, J.-R.; Gómez-García, C. J. *Chem. Commun*. **1997**, 1727 and references therein.

10.1021/cm990434x CCC: $18.00
Published on Web 11/09/1999

rence of the large 20-membered pores in indeed noteworthy.

Experimental Section

Synthesis and Initial Characterization. The zinc oxalates, **I** and **II**, were synthesized starting from a mixture containing 1,3-diaminopropane (DAP) and *n*-propylamine (PA), respectively, as the SDAs. For **I**, 1.273 g of oxalic acid was dissolved in 5 mL of deionized water and 0.41 g of ZnO was added to the above under constant stirring. To this mixture was added 0.42 mL of DAP and homogenized for 10 min. The final composition of the mixture was $ZnO{:}2H_2C_2O_4{:}$DAP:$55H_2O$. For **II**, zinc oxide, oxalic acid, PA, and water were mixed in the ratio $ZnO{:}H_2C_2O_4{:}2$PA:$55H_2O$ (all the chemicals used in the synthesis were obtained from Aldrich and used without further purification). The mixtures with an initial pH of 8.0 were transferred into a 23-mL (fill factor = 40%) PTFE bottle, and sealed in a stainless steel autoclave (Parr, Moline, IL). The sealed pressure bombs were heated at 110 °C for 168 h for **I** and 65 h for **II** under autogenous pressure. The mixtures after the reaction had a pH of 6.5. The evolution of acidity in the reaction mixture indicates that some of the amine molecules are consumed during the reaction. The resulting products, which contained a large quantity of transparent single crystals, were filtered and washed thoroughly with deionized water. Powder X-ray diffraction (XRD) patterns on the powdered crystals indicated that the products were new; the pattern is entirely consistent with the structure determined by single-crystal X-ray diffraction. Thermogravimetric analysis (TGA) was carried out in static air in the range between 25 and 600 °C using a heating rate of 10 °C/min.

Single-Crystal Structure Determination. A suitable single crystal of each compound was carefully selected under a polarizing microscope and glued to a thin glass fiber with cyanoacrylate (superglue) adhesive. Single-crystal structure determination by X-ray diffraction was performed on a Siemens Smart-CCD diffractometer equipped with a normal focus, 2.4 kW, sealed tube X-ray source (Mo Kα radiation, λ = 0.71073 Å) operating at 50 kV and 40mA. A hemisphere of intensity data was collected at room temperature in 1321 frames with ω scans (width of 0.30° and exposure time of 20 s per frame) in the 2θ range 3 to 48.0°. Pertinent experimental details for the structure determinations are presented in Table 1.

The structure was solved by direct methods using SHELXS-86[10] and difference Fourier syntheses. The amine molecule in **II** was heavily disordered and restraints for the bond distances have been used to keep the molecule intact and within reasonable limits. All the hydrogen positions for **I** were initially located in the difference Fourier maps, but for the final refinement, the hydrogen atoms were placed geometrically and held in the riding mode. No absorption corrections were applied. The last cycles of refinement included atomic positions for all the atoms, anisotropic thermal parameters for all the non-hydrogen atoms and isotropic thermal parameters for all the hydrogen atoms. Full-matrix-least-squares structure refinement against $|F^2|$ was carried out using SHELXTL-PLUS[11] package of programs. Details of the final refinements are given in Table 1. The final atomic coordinates and selected bond distances and angles for **I** are presented in Tables 2−4, and for **II** in Tables 5 and 6.

Table 1. Crystal Data and Structure Refinement Parameters for I, $[H_3N(CH_2)_3NH_3]^{2+}[Zn_2(C_2O_4)_3]^{2-}\cdot 3H_2O$ and II, $2[C_3H_7NH_3]^{+}[Zn_2(C_2O_4)_3]^{2-}\cdot 3H_2O$

	I	II
empirical formula	$Zn_2O_{15}C_9N_2H_{18}$	$Zn_2O_{15}C_{12}N_2H_{26}$
crystal system	triclinic	monoclinic
space group	$P\bar{1}$	$C2/c$ (no. 15)
crystal size (mm)	0.08 × 0.08 × 0.2	0.12 × 0.12 × 0.16
a (Å)	9.261(1)	15.847(1)
b (Å)	9.455(1)	9.685(1)
c (Å)	12.487(1)	18.333(1)
α (deg)	83.93(1)	90.0
β (deg)	88.01(1)	115.5(1)
γ (deg)	61.03(1)	90.0
volume (Å^3)	951.1(1)	2539.1(2)
Z	2	4
formula mass	524.8	569.1
ρ_{calc} (g cm^{-3})	1.83	1.60
λ (Mo Kα) (Å)	0.71073	0.71073
μ (mm^{-1})	2.60	1.97
θ range (deg)	1.64−23.29	2.46−24.03
total data collected	3984	5142
index ranges	$-10 \le h \le 9$	$-17 \le h \le 16$
	$-10 \le k \le 10$	$-10 \le k \le 7$
	$-13 \le l \le 12$	$-20 \le l \le 20$
unique data	2673	1849
observed data ($I > 2\sigma(I)$)	2561	1460
refinement method	full-matrix least squares on $\|F^2\|$	full-matrix least squares on $\|F^2\|$
R_{merg}	0.06	0.06
R indexes [$I > 2\sigma(I)$]	$R_1 = 0.03$	$R_1 = 0.07$
	w$R_2 = 0.08$	w$R_2 = 0.21$
R (all data)	$R_1 = 0.03$	$R_1 = 0.08$
	w$R_2 = 0.08$	w$R_2 = 0.22$
goodness of fit (S_{obs})	1.15	1.13
goodness of fit (S_{all})	1.15	1.05
no. of variables	278	125
largest difference map peak and hole (eÅ^{-3})	0.579 and −0.429	0.615 and −0.671

[a] $R_1 = \sum||F_0| - |F_c||/\sum|F_0|$. [b] $wR_2 = \{\sum [w(F_0^2 - F_c^2)^2]/\sum [w(F_0^2)^2]\}^{1/2}$. $w = 1/[\sigma^2(F_0)^2 + (aP)^2 + bP]$, $P = [\max.(F_0^2,0) + 2(F_c)^2]/3$, where $a = 0.0383$ and $b = 0.608$ for **I** and $a = 0.1597$ and $b = 0.0$ for **II**.

Results

$[H_3N(CH_2)_3NH_3]^{2+}[Zn_2(C_2O_4)_3]^{2-}\cdot 3H_2O$, I. The asymmetric unit of **I** contains 28 non-hydrogen atoms (Figure 1). **I** consists of macroanionic sheets of formula $[Zn_2(C_2O_4)_3]^{2-}$ with interlamellar $[H_3N(CH_2)_3NH_3]^{2+}$ ions, the individual layers involving a network of ZnO_6 octahedra and C_2O_4 units. Each Zn atom is cross-linked to six oxalate oxygens, forming a honeycomb network as shown in Figure 2a. This type of network results in a 12-membered pore within the layers, which stack one over the other, along the *c* axis. Such perforated sheets

(10) Sheldrick, G. M. *SHELXL-86 A program for the solution of crystal structures*; University of Göttingen: Göttingen, Germany, 1986.
(11) Sheldrick, G. M. *SHELXS-93 Program for Crystal Structures solution and refinement*; University of Göttingen: Göttingen, Germany, 1993.
(12) Thomas, J. M.; Jones, R. H.; Chen, J.; Xu, R.; Chippindale, A. M.; Natarajan, S.; Cheetham, A. K. *J. Chem. Soc., Chem. Commun.* **1992**, 929.
(13) Choudhury, A.; Natarajan, S.; Rao, C. N. R. *Chem. Mater.* **1999**, *11*, 2316.
(14) Estermann, M.; McCusker, L. B.; Baerlocher, Ch.; Merrouche, A.; Kessler, H. *Nature* **1991**, *352*, 320.
(15) Huo, Q.; Xu, R.; Li, S.; Ma, Z.; Thomas, J. M.; Jones, R. H.; Chippindale, A. M. *J. Chem. Soc., Chem. Commun.* **1992**, 875.
(16) Lin, H.-M.; Lii, K.-H.; Jiang, Y.-C.; Wang, S.-L. *Chem. Mater.* **1999**, *11*, 519. Choudhury, A.; Natarajan, S.; Rao, C. N. R. *J. Solid State Chem.* **1999**, *146*, 538.
(17) Neeraj, S.; Natarajan, S.; Rao, C. N. R. *Chem. Commun.* **1999**, 165; *New J. Chem.*, **1999**, *23*, 303; *Chem. Mater.* **1999**, *11*, 1390. Chidambaram, D.; Neeraj, S.; Natarajan, S.; Rao, C. N. R. *J. Solid State Chem.* **1999** in press.
(18) Gier, T. E.; Sticky, G. D. *Nature* **1991**, *349*, 508. Harrison, W. T. A.; Gier, T. E.; Moran, K. L.; Nicol, J. M.; Eckert, H.; Stucky, G. D. *Chem. Mater.* **1991**, *3*, 27. Nenoff, T. M.; Harrison, W. T. A.; Gier, T. E.; Stucky, G. D. *J. Am. Chem. Soc.* **1991**, *113*, 378. Feng, P.; Bu, X.; Stucky, G. D. *Angew. Chem., Int. Ed. Engl.* **1995**, *34*, 1745.
(19) Harrison, W. T. A.; Phillips, M. L. F. *Chem. Mater.* **1997**, *9*, 1837. Harrison, W. T. A.; Bircsak, Z. *Inorg. Chem.* **1998**, *37*, 3204 and references therein.
(20) Deyrieux, R.; Bero, C.; Penelous, A. *Bull. Soc. Chim. Fr.* **1973**, 25.

Table 2. Atomic Coordinates [× 10⁴] and Isotropic Thermal Parameters [Å × 10³] for the Non-hydrogen Atoms in I, $[H_3N(CH_2)_3NH_3]^{2+}[Zn_2(C_2O_4)_3]^{2-}\cdot 3H_2O$

atom	*x*	*y*	*z*	U_{eq}[a]
Zn(1)	5730(1)	−1446(1)	−2376(1)	30(1)
Zn(2)	2432(1)	−4895(1)	−2418(1)	30(1)
O(1)	3918(3)	603(2)	−3275(2)	38(1)
O(2)	5574(2)	353(2)	−1493(2)	36(1)
O(3)	7713(2)	−3357(2)	−1501(2)	36(1)
O(4)	7710(2)	−1502(2)	−3286(2)	32(1)
O(5)	5418(3)	−2980(2)	−3323(2)	36(1)
O(6)	3955(3)	−1833(3)	−1493(2)	38(1)
O(7)	2523(3)	−6710(2)	−3272(2)	35(1)
O(8)	4082(3)	−4397(3)	−3342(2)	37(1)
O(9)	447(2)	−4715(2)	−1492(2)	35(1)
O(10)	4264(3)	−6951(2)	−1520(2)	36(1)
O(11)	450(2)	−2954(2)	−3340(2)	34(1)
O(12)	2650(3)	−3282(3)	−1475(2)	35(1)
C(1)	4443(3)	−3452(3)	−2950(2)	27(1)
C(2)	3603(3)	−2791(3)	−1869(2)	27(1)
C(3)	9086(3)	−3650(3)	−1882(2)	27(1)
C(4)	9089(3)	−2610(3)	−2936(2)	27(1)
C(5)	3575(3)	1898(3)	−2898(2)	28(1)
C(6)	4561(3)	1761(3)	−1870(2)	28(1)
O(100)	7953(3)	−41(3)	4724(2)	43(1)
O(200)	1786(4)	−5377(3)	−5443(2)	52(1)
O(300)	2055(4)	577(4)	−175(3)	69(1)
N(2)	−1064(3)	3145(3)	−536(2)	38(1)
N(1)	−1312(3)	2251(3)	−4350(2)	43(1)
C(11)	−1915(4)	2160(4)	−3242(2)	43(1)
C(12)	−1069(4)	2591(4)	−2439(2)	41(1)
C(13)	−1851(4)	2722(4)	−1353(2)	44(1)

[a] *U*(eq) is defined as one-third of the trace of the orthogonalized U_{ij} tensor.

Table 3. Selected Interatomic Distances in I, $[H_3N(CH_2)_3NH_3]^{2+}[Zn_2(C_2O_4)_3]^{2-}\cdot 3H_2O$

moiety	distance (Å)	moiety	distance (Å)
Zn(1)−O(1)	2.087(2)	C(1)−O(5)	1.245(3)
Zn(1)−O(2)	2.068(2)	C(1)−O(8)	1.242(3)
Zn(1)−O(3)	2.082(2)	C(2)−O(6)	1.238(4)
Zn(1)−O(4)	2.105(2)	C(2)−O(12)	1.248(4)
Zn(1)−O(5)	2.093(2)	C(3)−O(3)	1.251(3)
Zn(1)−O(6)	2.104(2)	C(3)[b]−O(9)	1.245(3)
Zn(2)−O(7)	2.080(2)	C(4)−O(4)	1.251(3)
Zn(2)−O(8)	2.084(2)	C(4)[b]−O(11)	1.242(3)
Zn(2)−O(9)	2.084(2)	C(5)−O(1)	1.248(4)
Zn(2)−O(10)	2.095(2)	C(5)[a]−O(7)	1.249(3)
Zn(2)−O(11)	2.121(2)	C(6)−O(2)	1.249(3)
Zn(2)−O(12)	2.110(2)	C(6)[a]−O(10)	1.236(4)
C(1)−C(2)	1.566(4)	C(3)−C(4)	1.558(4)
C(5)−C(6)	1.559(4)		
	organic moiety		
N(1)−C(11)	1.484(4)	C(11)−C(12)	1.496(5)
C(12)−C(13)	1.503(4)	C(13)−N(2)	1.468(4)

[a] *x*, *y* − 1, *z*. [b] *x* − 1, *y*, *z*.

have been observed earlier in layered aluminophosphates[12] and iron phosphate−oxalates.[13] The protonated organic amine molecules sit in the middle of the 12-membered pores. There are three water molecules present in the material occupying the pores along with the amine (Figure 2b). Along the *b* axis the layers stack one over the other with the water molecules situated between the layers as shown in Figure 3. The amine and the water molecules participate in extensive hydrogen bonding, lending structural stability to this material. The various hydrogen-bond interactions between the sheets and the guest molecules can be seen in Figures 2b and 3. In Table 7, we list the important hydrogen-bond interactions.

Table 4. Selected Bond Angles in I, $[H_3N(CH_2)_3NH_3]^{2+}[Zn_2(C_2O_4)_3]^{2-}\cdot 3H_2O$

moiety	angle (deg)	moiety	angle (deg)
O(2)−Zn(1)−O(3)	95.9(5)	O(2)−Zn(1)−O(1)	80.0(3)
O(3)−Zn(1)−O(1)	173.2(2)	O(2)−Zn(1)−O(5)	169.3(2)
O(3)−Zn(1)−O(5)	93.5(2)	O(1)−Zn(1)−O(5)	91.0(2)
O(2)−Zn(1)−O(6)	95.4(3)	O(3)−Zn(1)−O(6)	93.7(4)
O(1)−Zn(1)−O(6)	92.1(3)	O(5)−Zn(1)−O(6)	79.0(2)
O(2)−Zn(1)−O(4)	93.0(2)	O(3)−Zn(1)−O(4)	79.8(2)
O(1)−Zn(1)−O(4)	94.8(4)	O(5)−Zn(1)−O(4)	93.5(3)
O(6)−Zn(1)−O(4)	169.9(2)	O(7)−Zn(2)−O(9)	94.0(2)
O(7)−Zn(2)−O(8)	98.0(2)	O(9)−Zn(2)−O(8)	164.5(4)
O(7)−Zn(2)−O(10)	80.1(2)	O(9)−Zn(2)−O(10)	96.6(2)
O(8)−Zn(2)−O(10)	95.1(2)	O(7)−Zn(2)−O(12)	172.5(3)
O(9)−Zn(2)−O(12)	89.3(4)	O(8)−Zn(2)−O(12)	79.9(4)
O(10)−Zn(2)−O(12)	92.9(2)	O(7)−Zn(2)−O(11)	95.3(1)
O(8)−Zn(2)−O(11)	89.3(2)	O(9)−Zn(2)−O(11)	79.9(1)
O(10)−Zn(2)−O(11)	174.1(2)	O(12)−Zn(2)−O(11)	91.9(2)
O(8)−C(1)−O(5)	126.8(2)	O(6)−C(2)−O(12)	126.6(3)
O(9)[a]−C(3)−O(3)	125.2(2)	O(11)[a]−C(4)−O(4)	126.6(2)
O(1)−C(5)−O(7)[b]	125.9(3)	O(10)[b]−C(6)−O(2)	127.2(2)
O(8)−C(1)−C(2)	117.1(2)	O(5)−C(1)−C(2)	116.1(2)
O(6)−C(2)−C(1)	116.6(2)	O(12)−C(2)−C(1)	116.8(3)
O(9)[a]−C(3)−C(4)	117.5(2)	O(3)−C(3)−C(4)	117.3(2)
O(4)−C(4)−C(3)	116.3(2)	O(11)[a]−C(4)−C(3)	117.1(2)
O(1)−C(5)−C(6)	116.8(2)	O(7)[b]−C(5)−C(6)	117.2(2)
O(10)[b]−C(6)−C(5)	116.7(2)	O(2)−C(6)−C(5)	116.1(2)
	organic moiety		
N(1)−C(11)−C(12)	112.2(3)	C(11)−C(12)−C(13)	111.6(3)
C(12)−C(13)−N(2)	113.7(3)		

[a] *x* + 1, *y*, *z*. [b] *x*, *y* + 1, *z*.

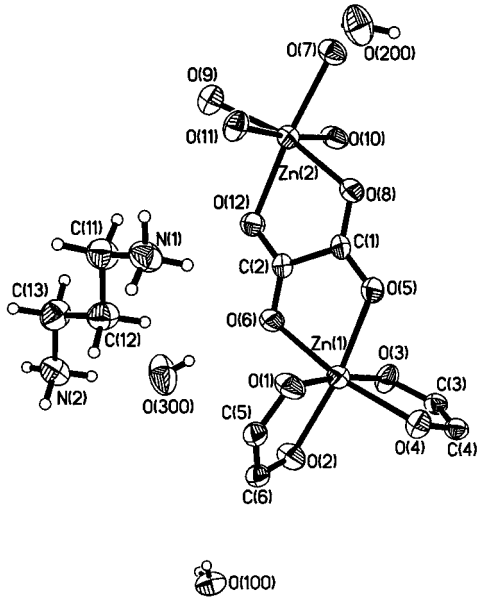

Figure 1. ORTEP plot of **I**, $[H_3N(CH_2)_3NH_3]^{2+}[Zn_2(C_2O_4)_3]^{2-}\cdot 3H_2O$. Thermal ellipsoids are given at 50% probability.

The Zn−O distances in **I** are in the range 2.068−2.121 Å (av 2.093 Å), with the longer distances being associated with the oxygens that are double-bonded to the carbon atoms. The variations in the distances are reflected in the C−O bonding, as well (Table 3). The O−Zn−O and O−C−O bond angles are in the range 79.9−173.2 and 125.2−127.2°, respectively (Table 4).

$2[C_3H_7NH_3]^{+}[Zn_2(C_2O_4)_3]^{2-}\cdot 3H_2O$ (II). The asymmetric unit of **II** contains 19 non-hydrogen atoms and is shown in Figure 4. The structure of **II** also consists of a network of ZnO_6 octahedra and oxalate units and three oxalate units connect with the Zn atoms, giving rise to a three-dimensional connectivity. Of the three

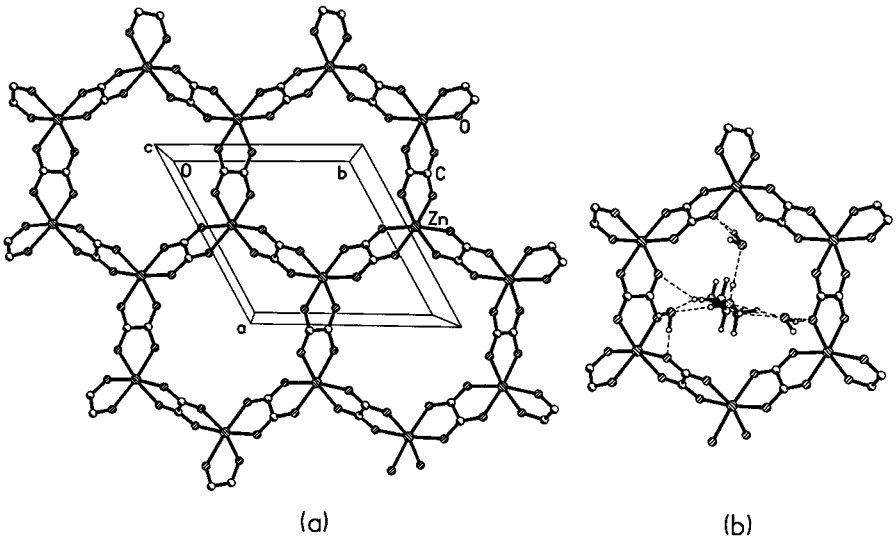

Figure 2. (a) Structure of **I**, $[H_3N(CH_2)_3NH_3]^{2+}[Zn_2(C_2O_4)_3]^{2-}\cdot 3H_2O$ in the *ab* plane showing the honeycomb architecture and (b) structure showing a single 12-membered aperture with the amine and water molecules. Dotted lines represent the hydrogen-bond interactions.

Table 5. Atomic Coordinates [× 10^4] and Isotropic Thermal Parameters [Å × 10^3] for the Non-hydrogen Atoms in II, $2[C_3H_7NH_3]^+[Zn_2(C_2O_4)_3]^{2-}\cdot 3H_2O$

atom	*x*	*y*	*z*	*U*(eq)[c]
Zn(1)	4180(1)	11249(1)	5861(1)	69(1)
O(1)	3584(3)	12847(5)	5024(3)	83(1)
O(2)	3936(3)	9650(5)	5025(2)	81(1)
O(3)	4669(3)	12626(4)	6827(2)	75(1)
O(4)	4662(3)	9861(4)	6835(2)	75(1)
O(5)	2783(3)	11145(4)	5688(3)	79(1)
O(6)	5408(3)	11355(4)	5687(3)	79(1)
C(1)	5000	12047(8)	7500	66(2)
C(2)	5000	10440(8)	7500	61(2)
C(3)	2273(4)	11993(6)	5192(3)	62(1)
C(4)	5425(3)	10499(6)	5193(3)	64(1)
O(100)[a]	4703(16)	14278(20)	4407(13)	394(10)
O(200)[a,b]	4644(14)	5548(18)	6795(11)	182(6)
O(300)[a,b]	4673(14)	6993(19)	6726(12)	189(6)
O(400)[a]	2801(13)	13183(19)	529(12)	360(9)
N(10)[a]	1721(12)	11247(10)	947(10)	222(6)
C(10)[a]	1738(18)	10745(28)	1735(12)	329(13)
C(11)[a]	2583(19)	11696(29)	2030(16)	347(13)
C(12)[a]	2645(18)	11158(19)	2833(15)	284(11)

[a] Refined isotropically. [b] Site occupancy factor (SOF) = 0.5. [c] *U*(eq) is defined as one-third of the trace of the orthogonalized U_{ij} tensor.

Table 6. Selected Bond Distances and Angles in II, $2[C_3H_7NH_3]^+[Zn_2(C_2O_4)_3]^{2-}\cdot 3H_2O$

moiety	distance (Å)	moiety	distance (Å)
Zn(1)−O(1)	2.096(4)	C(1)−O(3)	1.247(5)
Zn(1)−O(2)	2.093(4)	C(2)−O(4)	1.235(5)
Zn(1)−O(3)	2.082(4)	C(3)−O(1)[a]	1.250(7)
Zn(1)−O(4)	2.099(4)	C(4)−O(6)	1.237(7)
Zn(1)−O(5)	2.099(4)	C(4)−O(2)[b]	1.246(7)
Zn(1)−O(6)	2.105(4)	C(3)−O(5)	1.233(7)
C(1)−C(2)	1.557(12)	C(3)−C(3)[a]	1.554(10)
C(4)−C(4)[b]	1.559(10)		

moiety	angle (deg)	moiety	angle (deg)
O(3)−Zn(1)−O(2)	168.6(2)	O(3)−Zn(1)−O(1)	92.0(2)
O(2)−Zn(1)−O(1)	97.4(2)	O(3)−Zn(1)−O(4)	79.7(2)
O(2)−Zn(1)−O(4)	92.0(2)	O(1)−Zn(1)−O(4)	168.4(2)
O(3)−Zn(1)−O(5)	98.0(2)	O(2)−Zn(1)−O(5)	90.2(2)
O(1)−Zn(1)−O(5)	79.1(2)	O(4)−Zn(1)−O(5)	94.1(2)
O(3)−Zn(1)−O(6)	93.9(2)	O(2)−Zn(1)−O(6)	79.4(2)
O(1)−Zn(1)−O(6)	90.4(2)	O(4)−Zn(1)−O(6)	98.0(2)
O(5)−Zn(1)−O(6)	164.3(2)	O(3)[c]−C(1)−O(3)	126.5(7)
O(4)[c]−C(2)−O(4)	126.0(7)	O(5)−C(3)−O(1)[a]	126.5(5)
O(6)−C(4)−O(2)[a]	126.1(5)	O(3)−C(1)−C(2)	116.7(4)
O(4)−C(2)−C(1)	117.0(4)	O(5)−C(3)−C(3)[b]	118.0(6)
O(1)[a]−C(3)−C(3)[a]	115.5(6)	O(6)−C(4)−C(4)[b]	117.4(6)
O(2)[b]−C(4)−C(4)[b]	116.4(6)		

[a] $-x+1/2, -y+5/2, -z+1$. [b] $-x+1, -y+2, -z+1$. [c] $-x+1, y, -z+3/2$.

oxalate units, two connect via an *in-plane* linkage and the third one is cross-linked to the Zn atom in an *out-of-plane* manner resulting in a interrupted honeycomb structure with a 20-member elliptical ring, as shown in Figure 5. This type of connectivity between the Zn and oxalate units does not appear to have been encountered earlier. The elliptical pores in **II** formed by the linkage between 10 Zn and 10 oxalate units lying in the same plane and the other oxalate unit connect the elliptical pores such that two such rings are perpendicular to each other. Although the largest pore opening in **II** is a 20-membered one, it appears smaller in projection. Thus, along the *b* axis, the structure has the appearance of an 12-membered square-channel system made from 6 Zn and 6 oxalate units (~8.5 × 8.2 Å; longest atom−atom contact distance not including van der Waals radii) (Figure 6). The 20-member aperture has the dimensions ~17.2 × 6.9 Å. Along the *c* axis, it appears to have another 12-membered channel made from 8 Zn and 4 oxalate units of 8.3 × 6.1 Å diameter (Figure 7). The organic structure-directing agent, *n*-propylamine, which is highly disordered, occupies these channels along with water molecules. There is considerable hydrogen-bond interaction between the guest molecules and the host structure as presented in Table 7.

The Zn−O distances in **II** are in the range 2.068−2.121 Å (av 2.096 Å), with the longer distances being associated with the oxygens that are double-bonded to the carbon atoms. The O−Zn−O and O−C−O bond angles are in the range 79.1−168.4° and 126.0−126.5°, respectively (Table 6).

TGA studies of **I** and **II** were carried out in static air from room temperature to 600 °C and show weight loss in three steps. For **I**, a sharp mass loss of about 9.3%, occurring at 150 °C, corresponds to the loss of water molecules (calcd 10.3%) and a continuous two-step mass

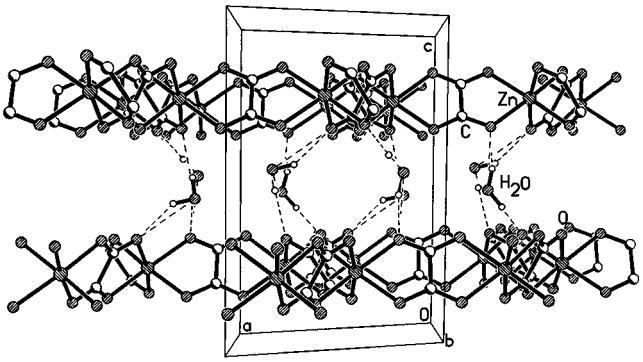

Figure 3. Structure of **I**, $[H_3N(CH_2)_3NH_3]^{2+}[Zn_2(C_2O_4)_3]^{2-}\cdot 3H_2O$ along the *ac* plane showing the layer arrangement. Amine molecules are not shown for clarity. Note that the water molecules involve in hydrogen bonding (dotted lines).

Table 7. Important Hydrogen-Bond Distances and Angles in Compounds I and II

moiety	distance, Å	moiety	angle (deg)
		I	
O(3)−H(11)	2.215(1)	O(3)−H(11)−N(2)	156.0(2)
O(12)−H(12)	1.957(1)	O(12)−H(12)−N(2)	178.2(1)
O(9)−H(11)	2.345(1)	O(9)−H(11)−N(2)	142.3(1)
O(4)−H(101)	1.930(1)	O(4)−H(101)−O(100)	175.4(2)
O(1)−H(102)	2.142(1)	O(1)−H(102)−O(100)	169.7(2)
O(7)−H(201)	2.063(1)	O(7)−H(201)−O(200)	160.6(1)
O(5)−H(202)	2.101(1)	O(5)−H(202)−O(200)	149.8(1)
O(2)−H(301)	2.166(1)	O(2)−H(301)−O(300)	175.0(1)
O(6)−H(302)	2.088(1)	O(6)−H(302)−O(300)	176.1(1)
O(100)−H(2)	1.964(1)	O(100)−H(2)−N(1)	167.7(3)
O(100)−H(3)	2.158(1)	O(100)−H(3)−N(1)	142.8(1)
O(200)−H(1)	1.887(3)	O(200)−H(1)−N(1)	164.2(1)
O(300)−H(10)	1.858(1)	O(300)−H(10)−N(2)	170.5(1)
		II	
O(6)−H(1)	2.342(1)	O(6)−H(1)−N(1)	132.6(1)
O(5)−H(2)	2.357(1)	O(5)−H(2)−N(1)	131.4(1)
O(100)−H(3)	2.424(1)	O(100)−H(3)−N(1)	158.2(1)

loss of 57.2% in the 300−400 °C region corresponds to the loss of carbon dioxide and amine molecules (calcd 55.6%). For **II**, a sharp mass loss of about 10.2% at 65 °C corresponds to the loss of water molecules (calcd 9.5%) and the mass loss of about 33.8% in the region 270−330 °C corresponds to the loss of carbon dioxide from the oxalate (calcd 33%), with the loss of 24.4% in the region 360−430 °C corresponding to the loss of the amine molecules (calcd 28%). The powder XRD patterns of the decomposed products indicated a poorly crystalline product with very weak reflections that corresponds to the mineral zincite, ZnO (JCPDS: 36-1451).

Adsorption studies, carried out gravimetrically with a Cahn electric balance, show that dehydrated **I** adsorbs water reversibly exhibiting a Langmuir type I adsorption isotherm (Figure 8). The observed weight changes at 25 °C correspond to 3.0 water molecules per unit cell, in agreement with the framework formula derived from crystallographic investigations. Unlike **I**, **II** loses crystallinity on desorption of water, indicating that the hydrogen-bond interactions between the water and the framework is crucial for the structural stability of this material. It is possible that such hydrogen bonding is responsible for the 20-membered aperture in **II**.

Discussion

Two new open-framework zinc oxalates, $[H_3N(CH_2)_3NH_3]^{2+}[Zn_2(C_2O_4)_3]^{2-}\cdot 3H_2O$ (**I**) and $2[C_3H_7NH_3]^{+}[Zn_2(C_2O_4)_3]^{2-}\cdot 3H_2O$ (**II**) have been synthesized by hydrothermal methods in the presence of amines. **I** and **II** are both members of a new family of framework solids with an identical framework composition. The difference in the structures of **I** and **II** arises from the distinct ways the oxalate units link to the Zn atoms. Whereas **II** has a three-dimensional structure arising from the covalent bonding between the oxalates and Zn, **I** has a two-dimensional architecture containing overlapping layers.

In **I**, the connectivity between the Zn and the oxalate moieties results in a 12-membered honeycomb aperture within the layer. The pores penetrate the entire structure in a direction perpendicular to the sheets, yielding a solid with unidimensional channels (~8.4 × 8.6 Å; longest atom−atom contact distance not including the van der Waals radii) containing the SDA and water molecules (Figure 2a,b). The type of perforated sheets seen in **I** is well-known in aluminum phosphates[12] and identical honeycomb structures have been known for $[M^{II}M^{III}(ox)_3]^-$ and $[M^{III}_2(ox)_3]$, where M is a transition element.[8,9] The honeycomb structures for the bimetallic transition metal oxalates have been made in the presence of ammonium cation. To our knowledge, this is the first case of a honeycomb structure in a pure zinc oxalate material. The honeycomb structure in **I** may be largely due to the use of the organic dication, $[DAPH_2]^{2+}$, in the starting synthesis mixture, as such a dication might be needed for neutralizing the charge on the dianionic oxalate sheets.

The layers formed by Zn and oxalate moieties in **I** are also present in **II**, except that the layers are cross-linked by another oxalate as can be seen from Figure 6. We also see large 20-membered apertures (Figure 5) formed by the Zn and the oxalate units. Large apertures are

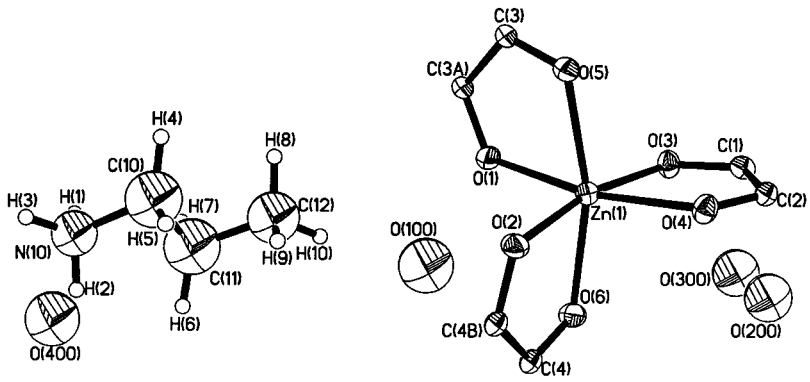

Figure 4. ORTEP plot of **II**, $2[C_3H_7NH_3]^{+}[Zn_2(C_2O_4)_3]^{2-}\cdot 3H_2O$. Thermal ellipsoids are given at 50% probability.

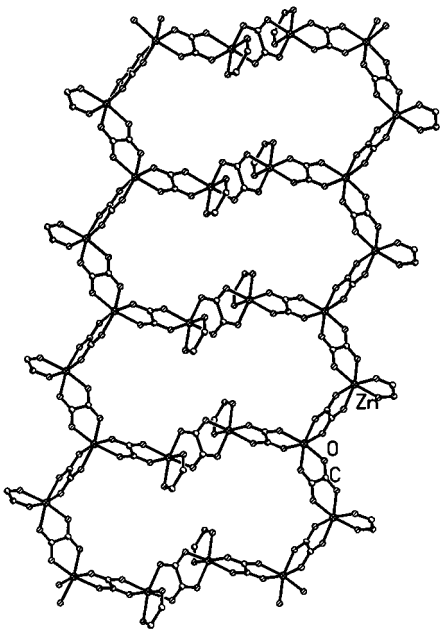

Figure 5. Structure of **II**, $2[C_3H_7NH_3]^+[Zn_2(C_2O_4)_3]^{2-}\cdot 3H_2O$, showing the 20-membered aperture. Note that the one of the Zn atoms is connected by out of plane oxalate unit.

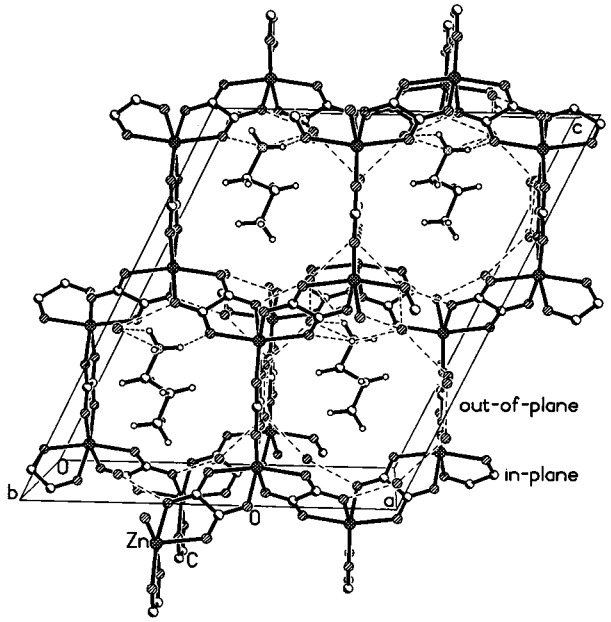

Figure 6. Structure of **II**, $2[C_3H_7NH_3]^+[Zn_2(C_2O_4)_3]^{2-}\cdot 3H_2O$, along the *b* axis showing the 12-membered square channels. Dotted lines represent the various hydrogen-bond interactions.

known to occur in other framework solids, including layered materials,[12,13] but 20-membered rings are indeed rare, such apertures and channels being found in very few materials.[14,15] A 20-membered aperture has, however, been observed recently in a Sn(II) oxalate,[7] possessing a layered architecture. In the layered Sn(II) oxalate, the 20-membered aperture results from linkages between 4- and 6-coordinated Sn(II) atoms and the oxalate units.[7] There is three-dimensional connectivity in **II** and yet, there are certain similarities between its structure and that of the Sn(II) oxalate. An examination of the connectivity patterns between the oxalates and M^{2+} ions (M = Zn or Sn) in both the solids reveals that **II** can be derived from the tin oxalate structure by the

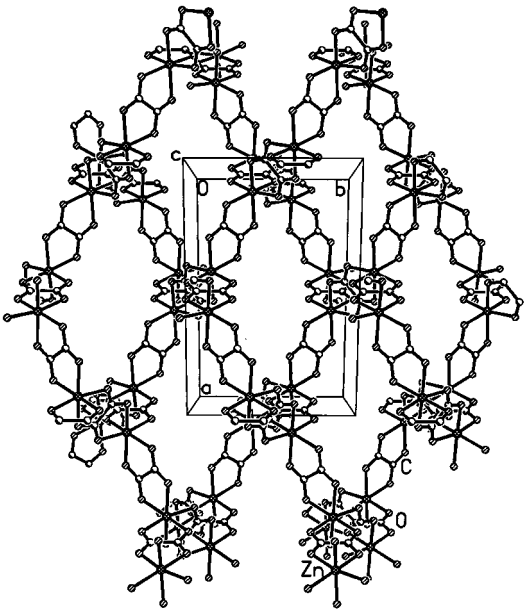

Figure 7. Structure of **II**, $2[C_3H_7NH_3]^+[Zn_2(C_2O_4)_3]^{2-}\cdot 3H_2O$, along the *c* axis showing the 12-membered elliptical channels.

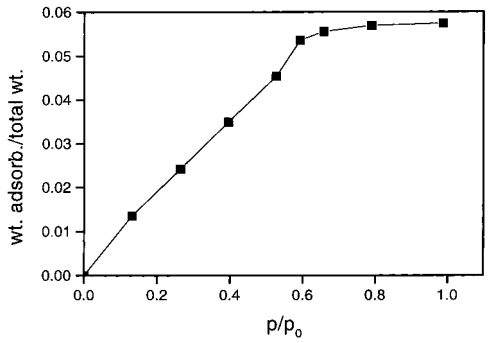

Figure 8. Room-temperature adsorption isotherm for H_2O in the dehydrated sample of **I**.

replacement of the 4-coordinated Sn(II) atoms by a 6-coordinated Zn atom having two in-plane connectivities and one out-of-plane connectivity with the oxalate units as shown in Figure 9. The out-of-plane connectivity is responsible for the three-dimensional nature of the structure (Figures 6 and 7). What is more interesting is the similarity between the structure of **II** and of the oxalate−phosphates discovered recently.[16] Thus, the Fe oxalate−phosphates have iron phosphate sheets cross-linked by oxalate units, not unlike the structure of an iron oxalate described by Decurtins et al.[8]

The importance of multipoint hydrogen bonding in these materials becomes apparent when we examine the distances and angles listed in Table 7. In **I**, which has a layered architecture with the organic amine at the center of the 12-membered ring along with the water molecules, hydrogen-bond interactions appear to be much stronger than in **II**, which has a more open structure. The primary hydrogen-bond interactions seem to be between the framework oxygens and water molecules. The amine molecules participate in both inter- (involving amine and framework) as well as intra- (involving amine and water molecules) layer hydrogen bonding. Compound **I** shows a dominance of hydrogen bonding with donor−acceptor (O···H) distances in the range of 1.85−2.35 Å and the majority of the angles

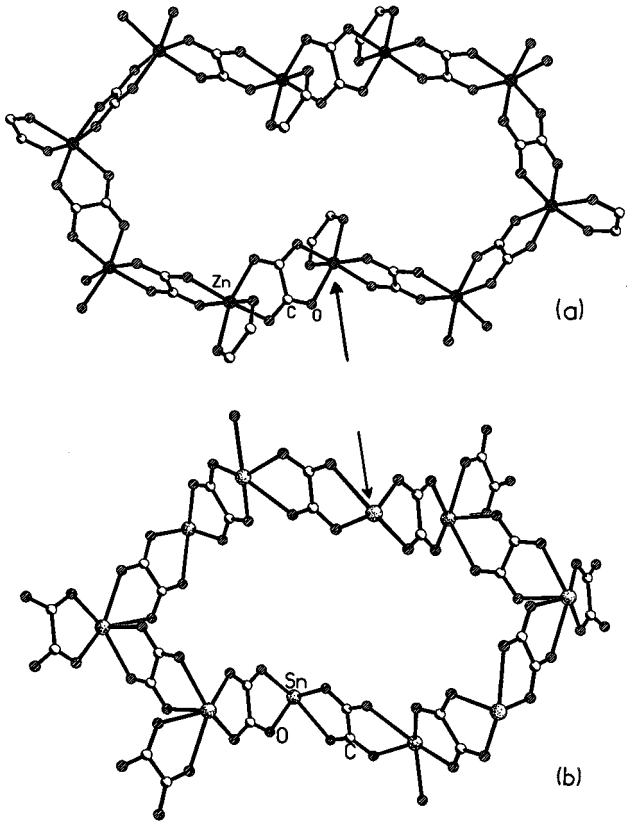

Figure 9. (a) Structure of **II**, $2[C_3H_7NH_3]^+[Zn_2(C_2O_4)_3]^{2-}\cdot 3H_2O$ showing a single 20-membered aperture and (b) structure of the tin(II) oxalate, $2[C(NH_2)_3]^+[Sn_4(C_2O_4)_5]^{2-}\cdot 2H_2O$ showing a single 20-membered aperture. Amine and water molecules are not shown for clarity. Note that the replacement of the four-coordinated Sn(II) (marked with an arrow) in b by a six-coordinate Zn (marked with an arrow) with two *in-plane* and one *out-of-plane* oxalate linkages gives rise to **II**.

above 150°. The ideal angle for a planar architecture is 180° and compound **I** with angles above 150° indicates the importance of hydrogen-bond interactions in low dimensional solids.

The coordination environment of Zn atoms in open-framework phosphates and oxalates provides an interesting comparison. The Zn atoms, in most of the zinc phosphates with open architectures have a tetrahedral environment (4-coordination).[17−19] In the oxalates under discussion, we have 6-coordination for the zinc atoms. This is probably because the average charge per oxygen on the oxalate (0.5) is less than that on the phosphate (0.75) and more oxalate oxygens are therefore needed to satisfy the valence of zinc.

Conclusions

The present study shows that new open-framework zinc oxalates can be obtained when the synthesis is carried out in the presence of organic amines. Of the two oxalates described here, one has a honeycomb structure and another an interrupted honeycomb structure. They possess a two-dimensional layer or three-dimensional channel structures, not unlike many of the Zn phosphates. While $Zn(C_2O_4)\cdot 2H_2O$ is known to possess a chain structure,[20] we are yet to obtain one-dimensional chain Zn oxalate analogues to chain phosphates in the presence of amines. The honeycomb structure observed by us for **I** is noteworthy as this is the first example of such an architecture for a divalent metal oxalate. This opens up the possibility of synthesizing oxalates of various divalent transition metals possibly possessing interesting magnetic properties. The interesting three-dimensional structure of **II** underscores the need for further research on open-framework oxalates prepared in the presence of structure-directing agents.

Acknowledgment. The authors thank Unilever plc for providing a research grant in support of our UCSB-JNCASR joint program.

CM990434X